Agrociencia

DEVELOPMENT AND EVALUATION OF A MULTI-CHAMBER ENVIRONMENTAL CONTROL SYSTEM

Raúl Alfonso **Rodriguez-Ruelas**[1], José Alfredo **Carrillo-Salazar**[1*], Juan Manuel **González-Camacho**[1], Nicacio **Cruz-Huerta**[1], Reyna Isabel **Rojas-Martínez**[1], Manuel **Livera-Muñoz**[1], Francisco **Carrasco-Hernández**[2], Noé **López-Martínez**[3]

[1]Colegio de Postgraduados Campus Montecillo. Carretera México-Texcoco km 36.5, Montecillo, Texcoco, State of Mexico, Mexico. C. P. 56264.
[2]Universidad Tecnológica de Durango. Carretera Durango–Mezquital km 4.5, Gabino Santillán, Durango, Mexico. C. P. 34308.
[3]Universidad Autónoma Chapingo. Departamento de Fitotecnia. Carretera México-Texcoco km 38.5, Chapingo, Texcoco, State of Mexico, Mexico. C. P. 56227.
* Author for correspondence: asalazar@colpos.mx

Citation: Rodriguez-Ruelas RA, Carrillo-Salazar JA, González-Camacho JM, Cruz-Huerta N, Rojas- Martínez RI, Livera-Muñoz M, Carrasco-Hernández F, López-Martínez N. 2024. Development and evaluation of a multi-chamber environmental monitoring system. **Agrociencia.** https://doi.org/ 10.47163/agrociencia.v58i7.3122

Editor in Chief: Dr. Fernando C. Gómez Merino

Received: November 28, 2023.
Approved: September 04, 2024.
Published in Agrociencia: October 22, 2024.

ABSTRACT

Growth chambers are control devices used in plant research. However, their high costs limit their application to a single environment, which compromises their efficiency for the generation of experimental data. The objective of this research was to design, construct, and assess the performance of a multi-chamber environmental control system capable of regulating both air temperature (*AT*) and relative humidity (*RH*). The evaluation was carried out using *Syngonium podophyllum* Schott plants. Three constant target temperature values (18, 23, and 40 °C) were established, together with a target RH value of 60 %. *AT* and *RH* data were recorded every 4 min for three days. The system was built with 15 growth chambers and the following devices: output (*AT*, *RH*, and lighting control), input (sensors), and central control managed by two Arduino® Mega 2560 based microcontrollers, plus a programmable logic controller. Programming was done in open-source languages such as Arduino® and Python®. Results indicate that the absolute error (*AE*) and standard deviation (*SD*) in *AT* were higher when the target temperature was lower (*AE* = 0.59 °C and *SD* = 0.93 °C) compared to the other higher target temperatures (*AE* = 0.31 °C and *SD* = 0.43 °C at 23 °C, and *AE* = 0.25 °C and *SD* = 0.51 °C at 40 °C). On the other hand, the *AE* in *RH* increased as temperature increased, going from *AE* = 3.75 % and *SD* = 5.12 % at 18 °C, to *AE* = 9.23 % and *SD* = 10.77 % at 40 °C. The use of open-source technologies allowed the construction of a multi-chamber environmental control system capable of replicating controlled environments.

Keywords: growth chamber, controlled environments, open source, control, *Syngonium podophyllum* Schott.

INTRODUCTION

Growth chambers are useful devices in basic and applied research, as they allow the regulation of the growth and development environment of plants (Mitchell, 2022).

These control variables include relative humidity, temperature, CO_2 level, and the quality and quantity of electromagnetic radiation, as well as photoperiod (Grindstaff *et al*., 2019). In addition, they are critical in intensive crop production infrastructure, such as in vertical farms within the framework of controlled environment agriculture (Mitchell, 2022).

In the field of agricultural research, agencies such as the National Aeronautics and Space Administration (NASA) have invested in the development of growth chambers to grow plants under extreme conditions (Reed and Vanden Bosch, 2023). They are also used in speed breeding research and in various areas of plant physiology, such as climate change, as well as in molecular biology (Bhatta *et al*., 2021; Jarvis *et al*., 2021; Dasgupta and Robinson, 2022; He *et al*., 2022). However, they are expensive (Cazzola *et al*., 2020), and usually only one growth chamber can be controlled at a time, whereas it would be desirable to be able to experiment with them in a more affordable, efficient, and extensive manner.

In response to this problem, some researchers have designed and built environmental control systems based on open-source technologies. For example, Padmanabha and Streif (2019) propose a low-cost programmable system for studies on organisms such as plants, fungi, and insect larvae using open-source technology. This system consists of modular units with sensors to measure gases and environmental properties, as well as relays to control lighting. On the other hand, Arunachalam and Andreasson (2022) present a remote monitoring system designed for plant experimentation. This system uses low-cost hardware components and open-source software, allowing data storage and automatic reconfiguration.

This work describes the physical components that make up a multi-camera environmental control system, including the structure, input, output, and control devices, as well as the programs used (user interface and code in Arduino®), based on open-source platforms. The objectives of this research were to design, construct, and evaluate a multiple environmental control system and to determine the accuracy and precision of the system for controlling the temperature and relative humidity of each growth chamber. The hypothesis was that technology based on open-source code such as Arduino® and Python® enables the design, construction, and operation of devices following the "do it yourself" concept. These tools make it possible to incorporate control algorithms from other authors easily and without copyright infringement issues (Fuller *et al.*, 2021; Marchus *et al*., 2022).

MATERIALS AND METHODS

The multi-chamber environmental control system was built inside a warehouse located in the facilities of the Postgraduate College Campus Montecillo, in Texcoco, State of Mexico, Mexico. The materials required for the construction of the system are available at the following link: https://github.com/Rodriguez-Ruelas/SISTEMA-DE-CONTROL-AMBIENTAL-MULTICAMARA

Design of the device

The system was designed to simultaneously control air temperature (*AT*, °C), relative humidity (*RH*, %), and photoperiod in 15 growth chambers, taking into account four of the six components required in environmental control systems for agricultural projects (Vatistas *et al*., 2022): thermal insulation, air conditioning (A/C) equipment, lighting, and the environmental control unit. However, control of CO_2 concentration and nutrient supply was not included in this design. Unlike other environmental control equipment, our approach provides air flow in each chamber using a single A/C source.

Physical components

The system is made up of four physical components: structure, control devices, input devices, and output devices (Figure 1).

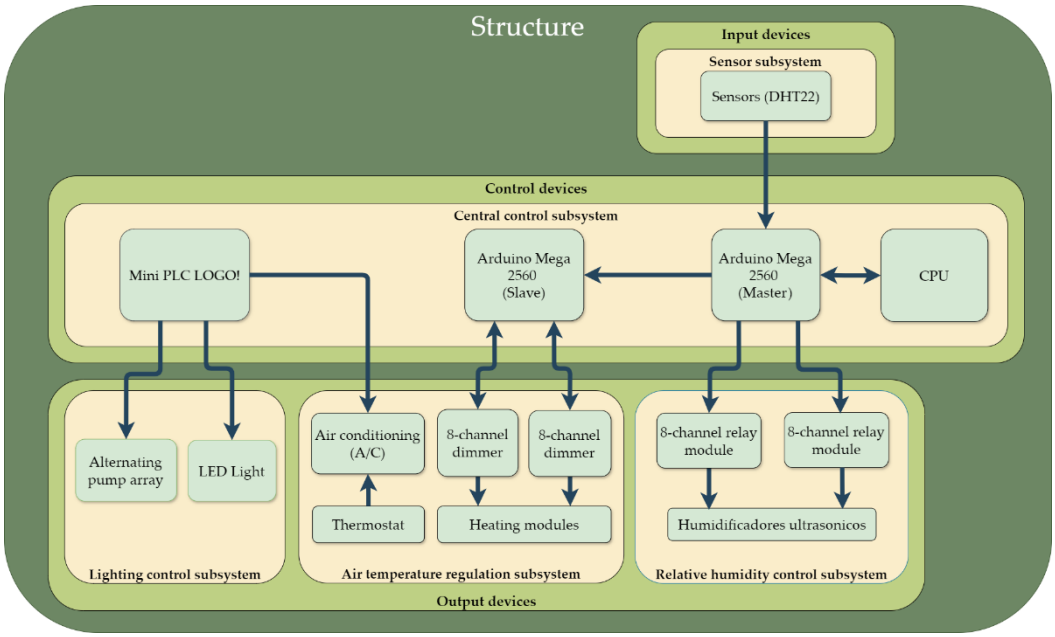

Figure 1. Physical components of the designed multi-chamber environmental control system, including input devices (sensors), output devices (air temperature (*AT*), relative humidity (*RH*), and lighting control subsystems), and central control devices (central control subsystem).

Control algorithms

The system operates through an application developed for the Windows® operating system. In addition, it includes two algorithms programmed in Arduino®, one for each microcontroller (master and slave), and the instructions for the programmable logic controller Mini PLC LOGO! (Siemens; Berlin, Germany) (Figure 2).

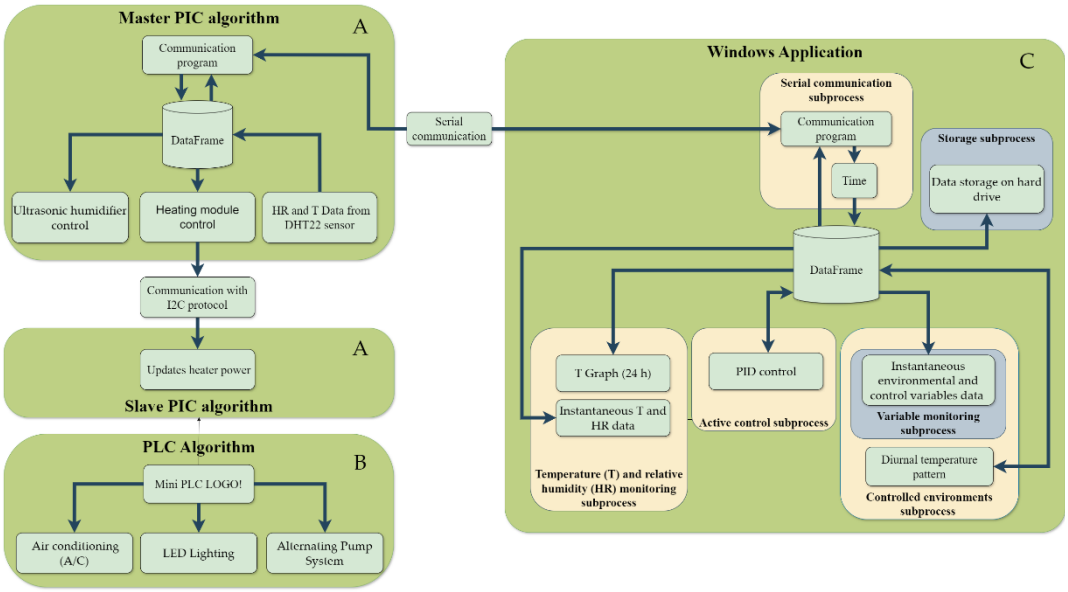

Figure 2. Flow chart of the control algorithms used in the multi-chamber environmental control system. A: Programmable integrated circuits (master and slave); B: programmable logic controller (Mini PLC LOGO!); C: graphical user interface.

Construction of the control system

Structure

The system consists of an angular iron frame with dimensions of 1.22 m long, 2.44 m wide, and 0.75 m high. The structure has 15 compartments or growth chambers organized in a 3 x 5 matrix arrangement. Each growth chamber was delimited with thermal insulation, forming a cube of 0.3 m per side (27 dm^3), excluding the volume of insulation. On the other hand, the lid was designed as a rectangular prism measuring 1.22 m in length, 2.44 m in width and 0.225 m in height. This cover serves several functions: it seals the growth chambers, serves as a base for fixing the lighting system, and acts as the outlet for the air coming from each growth chamber.

Central control subsystem

This subsystem has two microcontrollers: one master and one slave, based on the open-source Arduino® platform. The model used for both microcontrollers was the Mega2560 (Arduino; Ivrea, Italy), built from the ATmega2560 integrated circuit. The master microcontroller is connected to a computer (CPU) via a USB cable. It has 15 digital I/O ports configured as inputs for the DHT22 sensors and 16 digital I/O ports configured as outputs, connected to two mechanical relay modules to manage the switching on and off of the humidifiers. The slave microcontroller is connected to two

8-channel dimmer modules via 16 digital I/O ports configured as outputs. Attenuator modules are used to regulate the intensity of the AC voltage supplying the heating modules (Figure 4). The ignition of both the lighting subsystem and the alternating pumping arrangement for cooling the LEDs was managed by a programmable logic controller (Mini PLC LOGO!).

Sensor subsystem

A DHT22 sensor (Kuongshun Electronic; Shenzhen, China) was placed in each growth chamber to record *AT* and *RH* with an accuracy of ±0.5 °C and ±2 %, respectively. The resulting data were received by the master microcontroller.

Air temperature control subsystem

The *TA* regulating subsystem consists of two components: the cooling module and the heating module. The first consists of an LG® brand A/C unit with a capacity of 3516 kW. In addition, the subsystem has three 0.092 $m^3\ s^{-1}$ extractors (iPower; Beijing, China). A thermostat module with display (Steren; Mexico City, Mexico) was used to control the on/off of the compressor.

The heating module was constructed from a 10 cm ceramic insulating tube (No. 10). A 170 Ω nichrome wire resistor (0.1601 mm) was used to obtain an operation in the module from 0 to 127 V, with a maximum current of 0.74 A. The resistor was wound on a resistor holder constructed from ceramic insulating tube and attached to the inside of the tube by means of two screws with nuts that in turn serve the function of resistor pins. To withstand the high temperatures, the ceramic insulating tube was bonded with thermal silicone to a 25.4 mm coupling and a 25.4 mm hydraulic polyvinyl chloride (PVC) union nut.

The *AT* control process starts when the 16 °C air flow from the A/C coil passes through three lines of hydraulic PVC tubing (10.16 cm) and enters through the base of each chamber to the heating modules, where the air is heated to the target temperature (T_{Obj}). Each of these lines feeds five chambers, and the airflow in each line is regulated with a dimmer-operated exhaust fan RNL06-10Z (Leviton; New York, NY, USA). The hot air then exits through a duct located at the top of each chamber and is collected with 55 mm PVC pipe and released to the outside.

Relative humidity control subsystem

RH control was performed with 16 mm ultrasonic membrane humidifiers inside each growth chamber. This is important because the evaporator of the air conditioning system dehumidifies the air by cooling it (Daou *et al*., 2006).

Lighting control subsystem

A full-spectrum LED light chip for plant cultivation emitting 130 $\mu mol\ s^{-1}\ m^{-2}$ photosynthetic photon flux density at 380 nm (blue light) and 840 nm (red light) was installed in each growth chamber. The LEDs were fixed in copper tubing through

which water was recirculated with two 372.85 W peripheral pumps (Truper; Jilotepec, Mexico) that alternate their operation every 15 min to extract by conduction the heat produced by the LEDs and keep them within the operating temperature range. This cooling method is more efficient compared to the commercial solution of forced convection cooling (using a fan) with an aluminum heatsink attached to the back of the LED, which would increase the *AT* value surrounding the plants. In addition, cold air from the A/C was introduced through 10.16 cm tubing to the inside of the lid where the base of the LEDs is located.

Application for Windows

The application was programmed in Python® and PyQT5® languages. In addition, the simple-pid 1.0.1 library developed by Martin Lundberg, under license from the Massachusetts Institute of Technology (MIT), was used. This library implements a PID control (proportional (Kp), integrative (Ki), and derivative (Kd)) in each chamber in order to regulate the temperature. The Windows® application was installed on a desktop computer (CPU) and has two main functions: to establish bidirectional serial communication with the master microcontroller of the central control subsystem and to control environmental variables such as *AT* and *RH*. For this purpose, two user interfaces were designed: a window to monitor the current status and graphical records of the last 24 h of *RH* and *AT* in each growth chamber, and another interface to program the diurnal and nocturnal pattern of environmental variables. In particular, temperature programming can be performed using two options: maintaining a constant temperature or using an experimental curve, which consists of six set points.

Algorithms in Arduino

The programming of the Arduino® integrated circuits was performed in the Arduino IDE 2.2.1 development environment. The master microcontroller algorithm (Figure 2A) is responsible for establishing bidirectional serial communication with the Windows® application. Through this communication, the microprocessor algorithm receives the pulse width modulation (PWM, 0–255) values and the on/off status (0 or 1) of the humidifiers. It then provides the Windows application with the *AT* and *RH* values measured by the DHT22 sensors in each of the chambers. The master microcontroller also communicates with the slave microcontroller via the I2C (Inter-Integrated Circuit) protocol. Through this communication channel, the PWM values are transmitted to the attenuator modules to regulate the heating level.

PLC Algorithms

The Mini PLC (LOGO!) was programmed using LOGO! Soft Comfort V8.3. The algorithm is responsible for switching the water pumps on and off every 15 min, as well as switching the LEDs on and off.

Evaluation

Experimental conditions

In each growth chamber, a dwarf syngonium plant (*Syngonium podophyllum* Schott), selected because it is an adult plant of small size, was placed. Three constant target temperatures (T_{Obj}) were evaluated: 18, 23, and 40 °C, depending on the operating range of the equipment previously evaluated. The temperature of 23 °C was chosen because of its correspondence with the optimal growth range of dwarf syngnonium, which is between 22 and 25 °C (Salame and Zieslin, 1994; Chao *et al*., 2019). A photoperiod of 12 hours of light and 12 hours of darkness was maintained, with a target relative humidity (RH_{Obj}) of 60 %, which has been used as a standard for growth chamber evaluation (Jamhari *et al*., 2020). *AT* and *RH* data were recorded every 4 min for three days, for each chamber and T_{Obj}.

Evaluation metrics

Three hundred and sixty measurements per day were used to evaluate the precision and accuracy of *AT* and *RH* monitoring. The following statistical metrics were used: absolute error (*AE*) (Equation 1) and relative percent error (*RPE*) (Equation 2) to measure accuracy, and standard deviation (*SD*) (Equation 3) and coefficient of variation (CV, %) (Equation 4) to assess precision (Kokai *et al*., 2021).

$$AE = \sum_{i=1}^{n} |x_i - x_o| \tag{1}$$

where n is the total number of observations, x_i is the observed values, and x_o is the target value.

$$RPE = \sum_{i=1}^{n} \frac{|x_i - x_o|}{x_o} \tag{2}$$

$$SD = \sqrt{\frac{1}{n-1}\sum_{i=1}^{n}(x_i - \bar{x})^2} \tag{3}$$

where $\bar{x}$ is the arithmetic mean of the observed values.

$$CV = \left(\frac{SD}{\bar{x}}\right) \times 100\ \% \tag{4}$$

Similarly, the error (*ERR*) was calculated for the variables *AT* and *RH* (Equation 5). This analysis facilitated the identification of periods with positive or negative errors.

$$ERR_i = x_i - x_o \tag{5}$$

where ERR_i represents the error for the i-th observation.

The confidence interval (CI) for *AT* and *RH* was calculated using the following expression (Equation 6):

$$CI = \left(\bar{x} \mp Z_{\alpha/2}\frac{DS}{\sqrt{n}}\right) \tag{6}$$

where α is the significance level and $Z_{\alpha/2}$ is the critical value of the normal distribution.

RESULTS AND DISCUSSION

During the experimental phase, chambers 1 and 9 presented failures in the heater resistors, while chamber 5 had failures in the temperature sensor on the third day when the target temperature (T_{Obj}) was 40 °C. Because of this, the data corresponding to these chambers were eliminated (Table 1). Average air temperature values were recorded in the 15 chambers for three days, with T_{Obj} of 18, 23, and 40 °C (Table 1). When the target temperature was 18 °C, average maximum (chamber 10, day 1) and

Table 1. Average air temperature (°C) recorded during 24 h and its standard deviation (SD) in growth chambers with plants, evaluated at three target temperatures (n = 360 observations).

CN	18 °C			23 °C			40 °C		
	Day 1	Day 2	Day 3	Day 1	Day 2	Day 3	Day 1	Day 2	Day 3
2	18.47±0.98	18.05±0.28	18.39±0.62	22.97±0.44	22.95±0.42	22.86±0.52	39.83±0.29	39.63±0.61	39.66±0.69
3	18.64±1.22	18.04±0.25	18.54±0.76	23.02±0.32	23.01±0.28	23.00±0.26	40.02±0.38	40.02±0.30	39.97±0.62
4	18.93±1.83	18.02±0.12	18.58±0.84	23.00±0.26	23.02±0.26	23.00±0.20	39.97±0.38	40.00±0.24	39.99±0.47
5[†]	18.93±1.68	18.06±0.24	18.66±0.99	23.14±0.44	23.30±0.72	23.01±0.31	39.85±0.29	39.64±0.68	NA
6	18.25±0.62	18.01±0.21	18.18±0.34	23.00±0.39	23.00±0.35	23.01±0.30	40.01±0.26	40.01±0.28	39.98±0.59
7	18.29±0.73	18.00±0.15	18.15±0.38	22.99±0.21	23.00±0.20	23.03±0.25	40.01±0.10	40.00±0.11	39.96±0.52
8	18.67±1.16	18.09 ±0.40	18.55 ±0.87	23.04±0.47	23.04±0.53	23.01±0.47	40.04±0.45	40.01±0.36	40.12±0.86
10	19.00±1.70	18.04±0.19	18.63±0.91	23.16±0.46	23.24±0.60	23.00±0.18	39.90±0.34	40.00±0.40	39.98±0.61
11	18.42±0.90	18.02±0.19	18.30±0.53	22.96±0.53	22.92±0.54	22.80±0.65	39.83±0.50	39.91±0.46	39.77±0.79
12	18.68±1.20	18.08±0.27	18.58±0.84	23.00±0.32	23.02±0.39	22.93±0.49	40.00±0.12	39.95±0.19	39.91±0.67
13	18.69±1.26	18.04±0.39	18.55±0.89	23.03±0.56	23.02±0.57	23.00±0.59	40.00±0.27	39.98±0.31	39.93±0.81
14	18.96±1.59	18.09±0.28	18.76±1.05	23.05±0.41	23.09±0.49	23.03±0.42	40.00±0.19	40.00±0.15	39.92±0.67
15	18.46±1.00	18.01±0.19	18.27±0.56	22.98±0.31	23.01±0.30	23.05±0.32	39.69±0.48	39.55±0.69	39.84±0.72

CN: Chamber number; [†]: NA (value not available).

minimum (chamber 17, day 2) values of 19±1.7 and 18±0.15 °C, respectively, were observed, revealing a consistent deviation towards higher values. In contrast, at 23 and 40 °C, the maximum and minimum averages were 23.24±0.6 (chamber 10, day 2) and 22.8±0.64 °C (chamber 11, day 3), as well as 40.12±0.86 (chamber 8, day 3) and 39.55±0.69 °C (chamber 15, day 2), respectively.

Except when T_{Obj} was 18 °C, the error in *AT* increased during the light period, causing an increase of up to 6.5 °C (Figures 3A, 3B, and 3C). This behavior is attributed to the increase in daytime temperature outside the chambers, which generated an excessive demand on the air conditioning. On the other hand, when the chambers were set at T_{Obj} of 23 and 40 °C, it was found that the thermal disparity was less than 3 °C in some chambers (Figure 3), while in most of them the variations were less than 0.5 °C. Similarly, elevations or reductions of up to 2.5 °C were observed that were not necessarily associated with the light period (Figure 3).

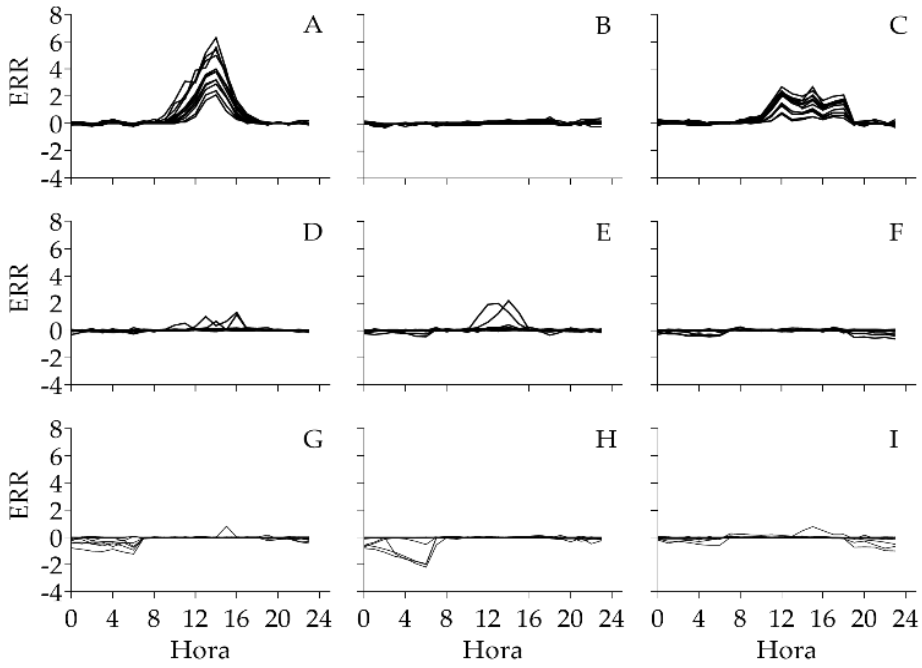

Figure 3. Error (*ERR*) between the target temperature (T_{Obj}) of 18 (A, B, and C), 23 (D, E, and F), and 40 °C (G, H, and I) and the air temperature (*AT*) in the growth chambers with plants, evaluated for three days.

The overall average *AT* plus its *SD* (23.02±0.43 °C) remained in the range of its respective T_{Obj} of 23±0.5 °C (Table 2). An improvement in the precision and accuracy of the system is observed as T_{Obj} increases (Table 2). Furthermore, the 95 % confidence interval (CI) for T_{Obj} confirms this trend, showing narrower intervals and higher precision with increasing T_{Obj}.

Table 2. Descriptive statistics of air temperature (*AT*) (n = 1080) recorded in growth chambers with plants evaluated at three target temperatures (T_{Obj}).

	18 °C	23 °C	40 °C
Mean	18.39	23.02	39.92
Standard deviation	0.93	0.43	0.51
CV (%)	5.05	1.88	1.00
Absolute error	0.59	0.31	0.25
Relative error (%)	3.20	1.36	0.69
CI (95 %)	18.37–18.40	23.01–23.02	39.91–39.93

CV: coefficient of variation; CI: confidence interval.

In relation to daily average relative humidity (*RH*), values greater than 60 % were frequently recorded when T_{Obj} was 18 °C, which contrasted with the results during tests with other T_{Obj}. On the other hand, there was evidence of a decrease in *RH* in the growth chambers as T_{Obj} increased (Table 3).

Table 3. Average relative humidity (*RH*) recorded during 24 h and its standard deviation (*SD*) in growth chambers with plants, evaluated at three target temperatures (n = 360 observations).

CN	18 °C			23 °C			40 °C		
	Day 1	Day 2	Day 3	Day 1	Day 2	Day 3	Day 1	Day 2	Day 3
2	63.03±3.83	59.88±2.61	60.26±2.50	59.80±2.70	59.26±2.54	58.57±2.70	59.87±3.06	59.60±3.47	58.89±2.98
3	60.73±4.03	55.44±4.92	55.96±5.01	53.64±4.03	51.13±4.85	47.82±5.09	46.55±3.94	40.09±80.10	40.73±3.96
4	58.09±6.90	51.59±6.07	52.34±6.70	59.61±2.93	53.33±6.70	44.67±6.87	47.17±8.18	43.43±11.82	31.48±3.79
5†	60.81±6.25	57.20±4.96	57.91±4.40	48.93±8.55	50.24±8.66	50.91±8.93	58.93±2.98	57.35±7.36	NA
6	60.45±3.90	54.74±4.88	56.44±5.75	54.39±4.12	50.88±4.74	47.36±5.02	43.12±3.86	36.51±6.87	35.11±2.93
7	63.01±3.39	59.64±4.13	60.00±3.54	58.70±4.33	59.42±2.33	59.35±2.82	55.09±3.85	48.21±6.06	44.28±4.47
8	62.33±5.16	59.83±4.17	60.01±3.76	57.00±8.15	60.37±3.67	59.83±3.20	56.16±10.91	56.45±8.59	44.34±12.86
10	60.15±4.87	57.84±3.86	57.87±3.82	49.46±7.16	45.19±5.77	48.09±6.28	59.1±2.76	45.34±11.15	32.95±3.36
11	61.75±3.69	59.59±2.89	60.01±2.41	56.22±4.16	56.66±4.13	57.11±3.98	55.92±5.22	49.82±12.34	56.15±5.93
12	63.11±3.12	60.87±2.76	60.91±3.08	60.84±3.20	60.47±3.16	59.69±3.50	60.75±3.32	60.72±3.37	61.04±3.07
13	61.78±3.99	57.24 ±4.02	56.80±4.28	57.12±2.92	56.10±3.28	54.67±4.06	59.01±1.22	57.70±2.20	43.36±6.27
14	61.38±4.18	56.12±4.36	56.22±4.79	56.17±3.36	54.61±3.69	52.51±4.24	57.65±3.44	58.21±3.33	56.73±4.09
15	62.29±3.73	58.75±3.20	59.35±3.04	59.21±3.38	58.70±3.75	57.70±4.08	60.31±40.00	59.68±3.77	59.73±3.61

CN: camera number; †: NA (value not available).

RH does not show a relationship with time of day (Figure 4). However, it is notable that as T_{Obj} increased, a corresponding increase in the magnitude of the error in *RH* was also observed. These errors, for the most part, remained below the RH_{obj} values, reflecting a consistent trend. In addition, a marked dispersion in *RH* values was observed between growth chambers, which was more evident as the T_{Obj} value increased.

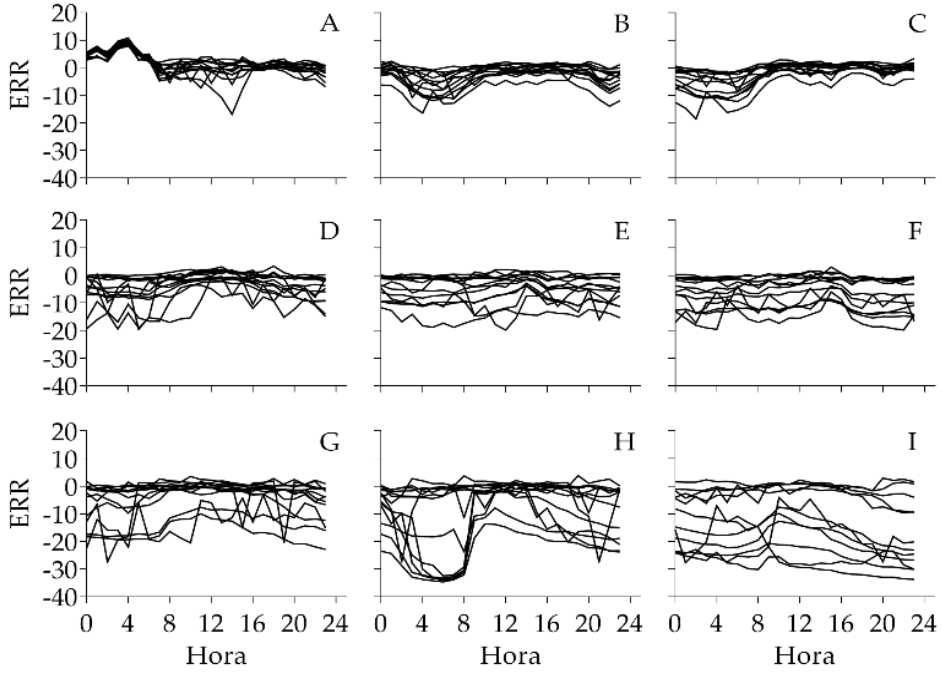

Figure 4. Error (*ERR*) between relative humidity (*RH*) and target relative humidity (RH_{Obj}) (60 %) in the 15 growth chambers with plants evaluated for three days at target temperatures of 18 (A, B, and C), 23 (D, E, and F), and 40 °C (G, H, and I).

The overall average *RH* decreases with increasing T_{Obj} (Table 4). This negative correlation is associated with a decrease in precision (increase in standard deviation (*SD*) and coefficient of variation (CV)) and accuracy (increase in absolute error (*AE*) and relative percent error (*RPE*)). In addition, the confidence interval (CI) increased as a function of T_{Obj}, and the maximum and minimum values in each confidence range moved away from the RH_{Obj} value (60 %). These results suggest the need to increase the

Table 4. Descriptive statistics of relative humidity (RH) (n = 1080) recorded in growth chambers with plants evaluated at three target temperatures.

	18 °C	23 °C	40 °C
Mean	59.02	55.03	51.57
Standard deviation	5.12	6.72	10.77
CV (%)	8.67	12.21	20.89
Absolute error	3.75	5.38	9.23
Relative error (%)	6.36	9.77	17.89
IC (95 %)	58.94–59.10	54.93–55.14	51.39–51.74

CV: coefficient of variation; IC: confidence interval.

humidification capacity of the air inside the growth chambers to maintain humidity as temperature increases.

The results indicate that external environmental conditions influence the ability of the system to regulate *AT* and *RH* in the growth chambers, this effect being more evident at T_{Obj} 18 °C, with greater absolute error during the light period. These results are similar to those of Porter *et al.* (2015), who evaluated multiple environmental variables in eight plant growth chambers (Conviron model BDW40 walk-in) and observed differences between daytime (24.5± 0.98 °C) and T_{Obj} (25 °C) temperatures. In addition, Hagopian *et al.* (2015) report a correlation between internal air temperature in environmental control systems and received solar irradiance. In this research, this could be due to diffuse solar radiation entering through skylights, which contributes to the increase in internal temperature in enclosed spaces. Therefore, it is necessary to improve the thermal insulation of the system.

Although the *AE* of the overall average *RH* at T_{Obj} 23 and 40 °C was considerable, it was observed that some chambers were able to reach the desired humidity level. The increased temperature in the chambers caused the expansion of the air inside, which increased the pressure and accelerated the outward flow of air. This air expansion resulted in a decrease of *RH* in the chamber, requiring the use of humidifiers with a higher water flow rate or a mechanism to regulate the air flow. In addition, this variability could be attributed to possible inconsistencies in the performance of ultrasonic humidifiers.

Another factor that influenced *RH* control was the drying of the air as it passed through the air conditioning (A/C) coil during the initial cooling phase, prior to entering the growth chambers. Katagiri *et al*. (2015) consider that the use of commercial humidifiers does not solve the problem of air dehumidification during the A/C cooling cycle in their environmental control equipment. Therefore, they opted to use an environmental cooling system with an air humidification mechanism to increase the humidity in the controlled atmosphere.

The system studied was stable at the evaluated temperatures of 18.38±0.67, 23.02±0.17, and 39.93±0.16 °C. The operating range exceeds the temperature limit of the "Advanced Plant Habitat" (APH) chamber, proposed by Massa *et al.* (2016), which is limited to temperatures of 18 to 30 °C. However, our system has a narrower thermal range compared to commercial equipment, such as the CARON© brand 7310, 7311, 7312, 7315, and 7317 models, which operate in a range of 15 to 45 °C and consist of a single chamber. A distinctive aspect of our proposal is its capacity to operate 15 cameras simultaneously. This arrangement translates into efficiency when evaluating plant performance in contrasting environments (Edet and Ishii, 2022). It also allows the implementation of diverse experimental designs, which is relevant given that environmental control systems cannot completely eliminate experimental error (Hammer and Hopper, 1997).

Unlike expensive commercial systems such as the Countertop model (Thermo Scientific™), which consists of a single compartment, our proposal offers a more

affordable solution, costing between $1661 and 2767 thousand USD, which represents only one-fifth of the value of commercial equipment. However, our multi-chamber environmental monitoring system has a limitation in the size of each chamber, which is 30 x 30 x 30 cm. This restricts evaluations to objects such as Petri dishes, test tubes, trays with microgreens, seedlings, or small-sized plants in 5 cm-high pots. It is important to note that both the configuration of the programs and the overall structure of the system can be adapted to control larger growth chambers.

CONCLUSIONS

The implementation of open-source technologies allowed the design and construction of a low-cost multi-chamber environmental control system. Despite operating in an unfavorable environmental setting, the system showed precision and accuracy in temperature control, although there were limitations in the regulation of relative humidity.

ACKNOWLEDGMENTS

The main author is grateful for the scholarship of the *Consejo Nacional de Humanidades, Ciencias y Tecnologías* (CONAHCYT) during his PhD, to the staff of the Plant Physiology Laboratory of the *Colegio de Postgraduados* for their invaluable support, and to the Plant Physiology Laboratory of *Universidad Autónoma Chapingo* for their collaboration and access to specialized equipment, which enriched our results.

REFERENCES

Arunachalam A, Andreasson H. 2022. RaspberryPi-Arduino (RPA) powered smart mirrored and reconfigurable IoT facility for plant science research. Internet Technology Letters 5 (1): e272. https://doi.org/10.1002/itl2.272

Bhatta M, Sandro P, Smith MR, Delaney O, Voss-Fels KP, Gutierrez L, Hickey LT. 2021. Need for speed: Manipulating plant growth to accelerate breeding cycles. Current Opinion in Plant Biology 60: 101986. https://doi.org/10.1016/j.pbi.2020.101986

Cazzola F, Bermejo CJ, Guindon MF, Cointry E. 2020. Speed breeding in pea (*Pisum sativum* L.), an efficient and simple system to accelerate breeding programs. Euphytica 216 (11): 178. https://doi.org/10.1007/s10681-020-02715-6

Chao Z, Yin-Hua S, De-Xin D, Guang-Yue L, Yue-Ting C, Nan H, Hui Z, Zhong-Ran D, Feng L, Jing S. 2019. *Aspergillus niger* changes the chemical form of uranium to decrease its biotoxicity, restricts its movement in plant and increase the growth of *Syngonium podophyllum*. Chemosphere 224: 316–323. https://doi.org/10.1016/j.chemosphere.2019.01.098

Daou K, Wang R, Xia Z. 2006. Desiccant cooling air conditioning: A review. Renewable and Sustainable Energy Reviews 10 (2): 55–77. https://doi.org/10.1016/j.rser.2004.09.010

Dasgupta S, Robinson EJZ. 2022. Attributing changes in food insecurity to a changing climate. Scientific Reports 12 (1): 4709. https://doi.org/10.1038/s41598-022-08696-x

Edet OU, Ishii T. 2022. Cowpea speed breeding using regulated growth chamber conditions and seeds of oven-dried immature pods potentially accommodates eight generations per year. Plant Methods 18 (1): 106. https://doi.org/10.1186/s13007-022-00938-3

Fuller S, Greiner B, Moore J, Murray R, van Paassen R, Yorke R. 2021. The python control systems library (python-control). *In* 2021 60th IEEE Conference on Decision and Control (CDC). Institute of Electrical and Electronics Engineers: Austin, TX, USA, pp: 4875–4881. https://doi.org/10.1109/cdc45484.2021.9683368

Grindstaff B, Mabry ME, Blischak PD, Quinn, M, Chris Pires J. 2019. Affordable remote monitoring of plant growth in facilities using Raspberry Pi computers. Applications in Plant Sciences 7 (8): e11280. https://doi.org/10.1002/aps3.11280

Hagopian WM, Schubert BA, Jahren AH. 2015. Large-scale plant growth chamber design for elevated pCO2 and δ13C studies. Rapid Communications in Mass Spectrometry 29 (5): 440–446. https://doi.org/10.1002/rcm.7121

Hammer PA, Hopper DA. 1997. Experimental design. *In* Langhans RW, Tibbitts TW. (eds.), Plant Growth Chamber Handbook. ISU: Ames, IA, USA, pp: 177–187.

He W, Pu M, Li J, Xu ZG, Gan L. 2022. Potato tuber growth and yield under red and blue LEDs in plant factories. Journal of Plant Growth Regulation 41 (1): 40–51. https://doi.org/10.1007/s00344-020-10277-z

Jamhari CA, Wibowo WK, Annisa AR, Roffi TM. 2020. Design and implementation of IoT system for aeroponic chamber temperature monitoring. *In* 2020 Third International Conference on Vocational Education and Electrical Engineering (ICVEE). Institute of Electrical and Electronics Engineers: Surabaya, Indonesia, pp: 1–4 https://doi.org/10.1109/icvee50212.2020.9243213

Jarvis BA, Romsdahl TB, McGinn MG, Nazarenus TJ, Cahoon EB, Chapman KD, Sedbrook JC. 2021. CRISPR/Cas9-Induced *fad2* and *rod1* mutations stacked with *fae1* confer high oleic acid seed oil in pennycress (*Thlaspi arvense* L.). Frontiers in Plant Science 12 (1664–462X): 652–669. https://doi.org/10.3389/fpls.2021.652319

Katagiri F, Canelon-Suarez D, Griffin K, Petersen J, Meyer RK, Siegle M, Mase K. 2015. Design and construction of an inexpensive homemade plant growth chamber. PLoS ONE 10 (5): e0126826. https://doi.org/10.1371/journal.pone.0126826

Kokai O, Kilbreath SL, McLaughlin P, Dylke ES. 2021. The accuracy and precision of interface pressure measuring devices: A systematic review. Phlebology 36 (9): 678–694. https://doi.org/10.1177/02683555211008061

Marchus CRN, Knudson JA, Morrison AE, Strawn IK, Hartman AJ, Shrestha D, Pancheri NM, Glasgow I, Schiele NR. 2022. Low-cost, open-source cell culture chamber for regulating physiologic oxygen levels. HardwareX 11: e00253. https://doi.org/10.1016/j.ohx.2021.e00253

Massa GD, Wheeler RM, Morrow RC, Levine HG. 2016. Growth chambers on the International Space Station for large plants. Acta Horticulturae 1134: 215–222. https://doi.org/10.17660/ActaHortic.2016.1134.29

Mitchell CA. 2022. History of controlled environment horticulture: Indoor farming and its key technologies. HortScience 57 (2): 247–256. https://doi.org/10.21273/hortsci16159-21

Padmanabha M, Streif S. 2019. Design and validation of a low cost programmable controlled environment for study and production of plants, mushroom, and insect larvae. Applied Sciences 9 (23): 5166. https://doi.org/10.3390/app9235166

Porter AS, Evans-Fitz GC, McElwain JC, Yiotis C, Elliott-Kingston C. 2015. How well do you know your growth chambers? Testing for chamber effect using plant traits. Plant Methods 11 (1): 44. https://doi.org/10.1186/s13007-015-0088-0

Reed DW, Vanden Bosch CA. 2023. Engineering perspectives of growing plants in space. Journal of the Indian Institute of Science 103 (3): 797–805. https://doi.org/10.1007/s41745-023-00369-6

Salame N, Zieslin N. 1994. Peroxidase activity in leaves of *Syngonium podophyllum* following transition from *in vitro* to *ex vitro* conditions. Biologia Plantarum 36 (4): 619–622.

Vatistas C, Avgoustaki DD, Bartzanas T. 2022. A systematic literature review on controlled-environment agriculture: How vertical farms and greenhouses can influence the sustainability and footprint of urban microclimate with local food production. Atmosphere 13 (8): 1258. https://doi.org/10.3390/atmos13081258